RESEARCH ARTICLE

Box-Behnken Design Optimization of Captopril-Loaded Transferosomes: Formulation and Characterization

Ismail Y[1], Mrunalini Harish Kulkarni[2*], Yamjala Ganesh Kumar[3], G Dharmamoorthy[4]

[1]Crescent School of Pharmacy, B.S.Abdur Rahman Crescent Institute of Science and Technology, Chennai, Tamil Nadu, India.

[2]School of Pharmacy, Vishwakarma University, Kondhwa,Pune, India.

[3]Sree Dattha Institute of Pharmacy, Department of Pharmacognosy & Phytochemistry, Sheriguda, Ibrahimpatnam, Rangareddy, Telangana, India.

[4]Dept. of Pharmaceutical Analysis, MB School of pharmaceutical sciences (Erstwhile Sree Vidyanikethan college of pharmacy), Mohan Babu University, Rangampeta, Tirupati, Andhra Pradesh, India.

Received: 16th March, 2024; Revised: 23rd May, 2024; Accepted: 02nd August, 2024; Available Online: 25th September, 2024

ABSTRACT

This study aimed to overcome the limitations of oral delivery and enhance the permeation of Captopril (CPL) by developing transferosomes. Transferosomes encapsulating CPL were prepared using a thin film hydration method. Seventeen formulations were prepared, varying Soya lecithin, Tween-20, and sonication speed. The formulations were evaluated for vesicle size (VS), polydispersity index (PDI), and entrapment efficiency (EE%). The optimized formulation's discharge profile was compared with that of the CPL suspension. Transferosomes exhibited VS ranging from 244 to 376 nm and EE% from 65 to 91%, with zeta potentials ranging from -51 to -26 MV. *In-vitro* and *ex-vivo* permeation studies demonstrated superior drug permeation for transferosomal formulations compared to plain CPL suspension. CPL transferosomes represent a promising delivery system for prolonged and controlled drug discharge, offering potential improvements in hypertension management.

Keywords: Captopril, Drug permeation, Delivery, Transdermal, Transferosomes.

International Journal of Drug Delivery Technology (2024); DOI: 10.25258/ijddt.14.3.06

How to cite this article: Ismail Y, Kulkarni MH, Kumar YG, Dharmamoorthy G. Box-Behnken Design Optimization of Captopril-Loaded Transferosomes: Formulation and Characterization. International Journal of Drug Delivery Technology. 2024;14(3):1292-1298.

Source of support: Nil.

Conflict of interest: None

INTRODUCTION

Heart failure presents a formidable challenge in public health globally. This chronic complaint frequently arises from coronary artery disease, hypertension, and myocardial infarction, and -proceeds to symptoms like fatigue, dyspnea, edema, and exercise intolerance, profoundly affecting patients' quality of life. Multiple mechanisms contribute to heart failure, including impaired contractility, increased afterload, and neurohormonal activation, with systems like the renin-angiotensin-aldosterone system and sympathetic nervous system playing pivotal roles, inducing vasoconstriction, sodium and water retention, and adverse cardiac remodeling. Management of heart failure involves a multifaceted approach targeting symptom alleviation, functional improvement, and morbidity and mortality reduction. Pharmacological interventions, including ACE inhibitors, β-blockers, diuretics, and device-based therapies, are central to treatment, alongside lifestyle modifications and dietary sodium restriction. Despite treatment advances, heart failure remains associated with high rates of hospitalization, mortality, and healthcare costs.[1] Thus, ongoing research focuses on identifying novel therapeutic targets, optimizing treatment strategies, and enhancing patient outcomes through early diagnosis, comprehensive patient education, and multidisciplinary care.[2-5]

Transdermal drug delivery is the expedient route for directing therapeutic agents, bypassing the oral route's limitations, such as first-pass metabolism and gastrointestinal irritation. This approach involves delivering drugs across the skin's outermost layer, the stratum corneum, into the systemic circulation, providing sustained and controlled discharge for improved efficacy and patient compliance.[6] Transdermal patches, gels, creams, and microneedle-based systems are among the formulations used in transdermal delivery, offering advantages such as prolonged drug discharge, condensed systemic side effects, and avoidance of gastrointestinal degradation. Various factors influence transdermal drug absorption, including drug physicochemical properties, formulation composition, skin integrity, and

*Author for Correspondence: mrunalini.kulkarni@vupune.ac.in

application site. Enhancing permeation through strategies like chemical permeation enhancersm,[7-9] physical methods such as iontophoresis and electroporation, and innovative delivery systems like nanoparticles and vesicular carriers continue to advance transdermal drug delivery, expanding its applications across diverse therapeutic areas from pain management and hormone replacement to cardiovascular and central nervous system disorders. Despite its potential, challenges such as limited drug permeability, skin irritation, and variability in absorption rates persist, necessitating ongoing research to optimize formulations, enhance skin penetration, and ensure safety and efficacy in clinical practice.[10]

Transferosomes, a type of elastic vesicular carrier, hold promise as efficient drug delivery systems for transdermal applications. Composed of phospholipids and edge activators like surfactants, these vesicles possess a flexible lipid bilayer structure that allows them to deform and squeeze through skin pores, enhancing drug penetration into deeper skin layers and systemic circulation. The unique flexibility of transferosomes enables them to adapt to the stratum corneum's irregularities, facilitating drug permeation across the skin barrier. This characteristic makes them particularly suitable for delivering both hydrophilic and lipophilic drugs with varying molecular weights.[11-14] Their ability to improve drug bioavailability, provide sustained discharge, and minimize local irritation makes them attractive candidates for transdermal drug delivery, especially for medications with poor oral bioavailability or those requiring controlled discharge profiles. Research continues to explore novel formulations, optimization strategies, and innovative techniques to harness the full potential of transferases in enhancing drug delivery efficiency and therapeutic outcomes across various medical conditions.[15]

Captopril (CPL) is an ACE inhibitor and is a widely prescribed medication for managing hypertension. CPL inhibits the breakdown of bradykinin, a vasodilator, further contributing to its antihypertensive effects.[16] Beyond hypertension. Its rapid onset of action and short duration make it suitable for acute hypertension treatment, while its long-term use has been shown to improve outcomes and reduce mortality in heart failure patients. Common adverse effects include hypotension, hyperkalemia, dry cough, and angioedema, particularly in patients with a history of allergic reactions. Despite these side effects, CPL remains a cornerstone therapy in the management of cardiovascular diseases due to its proven efficacy and cost-effectiveness. Ongoing research continues to explore its therapeutic potential in various other conditions, highlighting its significance in modern medicine.[17,18]

This study aims to make CPL transferases utilizing the Box-Behnken design method with the aid of Design Expert software. The aim is to investigate the influence of key factors such as soya lecithin, Tween-20, and sonication time on crucial parameters, including VS, EE, and ZP of CPL transferosomes. Through systematic experimentation and optimization, the study seeks to enhance the efficiency and effectiveness of CPL delivery via transferosomal carriers, offering potential advancements in drug delivery technology for improved therapeutic outcomes.

MATERIALS AND METHODS

Materials

Captopril, generously supplied by Zydus Medica, Ahmedabad, served as the primary pharmaceutical ingredient in this study. Soya lecithin, Tween-20, and polyethylene glycol (PEG) 400 were procured from Fischer Chemicals. All other reagents utilized in the experimentation were of AR grade.

Preparation of transferosomes

Soya lecithin and Tween-20 were dissolved in a mixture of chloroform and ethanol, with a ratio of 2:1, followed by the removal of the solvent using rotary evaporation at 60 RPM/min for 15 minutes. To ensure complete elimination of any residual solvent, the lipid films were subjected to overnight vacuum drying. The resulting lipid films were then reconstituted by hydrating them with 10 mL of PBS (pH 6.8), containing the desired drug. This hydration process involved rotating the mixture for 45 minutes.[19] The transfersomal suspension obtained was stored under refrigerated conditions at 4°C. A total of 17 formulations were prepared using the Box Behnken Design method, facilitated by Design Expert software (Table 1).

Compatibility studies by DSC and FTIR

To evaluate the compatibility between the drug and polymers, samples were judged by DSC. The drug alone and its combination with the excipient were heated from 30 to 300°C. DSC analysis is a common technique for assessing the thermal behavior of materials, enabling the detection of interactions

Table 1: Composition of CPL transferosomes

Trials	*Independent variables*			*Dependent variables*					
				Observed response			*Predicted response*		
	X_1	X_2	X_3	Y_1	Y_2	Y_3	Y_1	Y_2	Y_3
CT-1	75	10	70	347	75	-33	236.37	79.00	-36.25
CT-2	95	10	70	363	73	-35	269.80	85.60	-47.40
CT-3	75	30	70	237	91	-51	255.12	82.50	-37.38
CT-4	95	30	70	381	65	-26	251.75	90.50	-49.88
CT-5	75	20	60	277	77	-40	269.80	85.60	-47.40
CT-6	95	20	60	376	67	-29	242.62	67.00	-26.50
CT-7	75	20	80	244	79	-36	378.12	65.50	-29.13
CT-8	95	20	80	232	69	-27	377.50	66.50	-25.62
CT-9	85	10	60	371	66	-30	269.80	85.60	-47.40
CT-10	85	30	60	310	89	-43	269.80	85.60	-47.40
CT-11	85	10	80	251	81	-38	348.25	73.50	-36.13
CT-12	85	30	80	265	70	-28	257.88	70.50	-28.88
CT-13	85	20	70	262	83	-46	266.37	79.00	-40.50
CT-14	85	20	70	251	90	-47	305.88	87.50	-43.63
CT-15	85	20	70	281	84	-45	350.50	73.50	-33.37
CT-16	85	20	70	257	86	-49	269.80	85.60	-47.40
CT-17	85	20	70	298	85	-50	383.63	67.00	-28.75

X_1: Soya lecithin; X_2:Tween-20; X_3:Sonication time Y_1: Vesicle size; Y_2:EE; Y_3: Zeta potential and compatibility between components. By comparing the thermal profiles of the drug alone and in combination with the excipient, any changes in melting points, enthalpy, or other thermal parameters can be observed, indicating potential interactions. This method provides valuable insights into the suitability of polymers for formulating the drug and ensuring the stability and efficacy of the final product.

Further, Fourier Transform Infrared (FTIR) spectroscopy was employed. The IR spectra were captured utilizing a spectrophotometer over a wavelength range spanning from 4000 to 400 cm^{-1}. This analytical approach helps to analyze chemical bonds and efficient groups present in both the drug and the polymers, thereby determining their compatibility.

Optimization of CPL transferosomes by Box Behnken design

In this investigation, the impact of Soya lecithin and Tween-20 on CPL-loaded transferosomes (CT) was analyzed utilizing a 3^3 Box-Behnken design. Employing Design-Expert software, 17 experimental runs were generated, implementing a nonlinear quadratic model equation.[20-23] The model considered various coefficients, including linear, interaction, and quadratic, along with the intercept. Independent variables (IV), i.e., soya lecithin (X_1), tween-20 (X_2), and sonication time (X_3) were studied against dependent variables (DV), including vesicle size (VS) (Y_1), entrapment efficiency (EE) (Y_2), and zeta potential (ZP) (Y_3).

Description of VS, PDI, and ZP

To characterize the CT, various analyses were performed to assess its stability and behavior. The VS and surface charge were evaluated by diluting a sample of the CT with double-distilled water to ensure optimal measurement conditions. The measurements for VS and ZP were then conducted using a laser scattering particle size analyzer.[24-26]

Entrapment efficiency

To assess the drug entrapment efficiency (DEE) of CT, ultracentrifugation is conducted initially at 20,000 rpm and 10°C for 30 minutes. Later, 1 mL of CT is extracted and mixed with 9 mL of PBS (pH 7.4). The absorbance of the diluted supernatant is then analyzed at 254 nm using a UV–vis spectrophotometer (Thermo Spectronic UV-1, USA). The DEE is calculated using the formula (Eq.1).[27,28]

$$DEE\ (\%) = \frac{(Total\ amounnt\ of\ cilnidipine - Free\ amount\ of\ cilnidipine)}{Total\ amounnt\ of\ cilnidipine} X100 \quad (1)$$

RESULTS AND DISCUSSION

Compatibility results

The analysis of DSC thermograms provided valuable insights into the interaction between CPL and excipients, shedding light on their compatibility and potential formulation benefits. CPL exhibited a distinct endothermic peak at 109.42°C, while the combination with excipients displayed a peak at 103.87°C. The observed leftward shift in the thermograms indicates efficient interaction between CPL and excipients, suggesting good miscibility. This alteration in peak temperature signifies changes in the thermal properties of the drug-excipient mixture, further confirming their compatibility. Overall, these findings support the notion of effective interaction between CPL and excipients, which is crucial for formulating stable and efficient drug delivery systems (Figure 1).

The FTIR analysis discovered that the specific peaks and stretches existing in the FTIR spectrum of CPL remained unaltered even when combined with the excipients (Figure 2). This indicates that the interactions between CPL and the excipients did not induce significant changes in the chemical structure or functional groups of the drug. The preservation of these characteristic peaks suggests that the excipients were compatible with CPL and did not cause any discernible chemical modifications or interactions that could compromise its molecular integrity. This underscores the suitability of the excipients for formulating CPL-based products while preserving its pharmaceutical properties.

VS, PDI, and ZP results

The transferosomes demonstrated a range of vesicular sizes from 244 to 376nm, indicating variability in the size distribution within the formulation. Additionally, the EE% ranged from 65 to 91%, suggesting differences in the effectiveness of encapsulating the drug within the vesicles across various formulations. Furthermore, the ZPs ranged from -51 to -26MV, indicating the surface charge of the

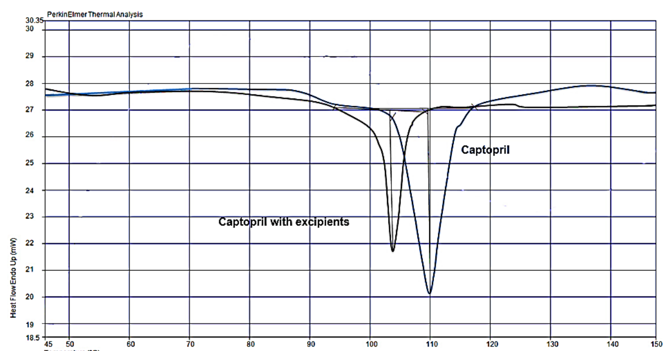

Figure 1: DSC thermograms of CPL individually and along with excipients

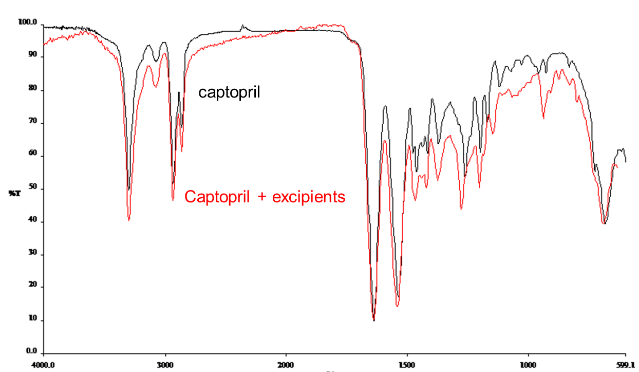

Figure 2: FTIR spectrum of CPL alone and its combination with excipients used

transferosomes and their potential stability in solution. These findings highlight the heterogeneity in size, drug entrapment, and surface charge characteristics among the transferosome formulations, which may influence their performance and suitability for drug delivery applications.

The Polydispersity Index (PDI) depicted in Figure 3 delivers valuable visions into the uniformity of particle sizes within the transferosomes. A PDI value approaching zero signifies a narrow size distribution, indicating predominantly uniform particle sizes. This uniformity is crucial for consistent drug delivery and efficacy, as it ensures that most particles are of similar sizes, leading to predictable performance. However, a higher PDI suggests a broader range of particle sizes, indicating greater variability within the formulation. This variability may pose challenges in achieving uniform drug distribution and could impact the overall performance of the formulation. Therefore, monitoring and optimizing the PDI of transferosome formulations are essential steps in ensuring their effectiveness for drug delivery applications (Figure 4).

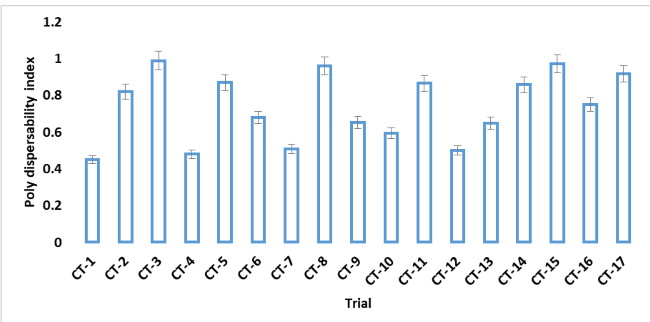

Figure 3: Poly dispensability index of the transferosomes

Effect of IV on the Responses

The Model F-value of 13.6 represents the model's significance, with a mere 0.12% probability that such a higher F-value could occur due to noise, affirming its validity. Significant model terms, including A, B, AB, AC, BC, A^2, B^2, and C^2, with *p-values* < 0.05, underscore their importance. The Lack of Fit F-value of 0.83, insignificance relative to pure error, and a 54.11% chance due to noise suggest a well-fitting model capable of capturing underlying relationships. Both the Predicted R^2 (0.6151) and adjusted R^2 (0.8764) are in reasonable agreement, indicating consistent predictive power across datasets. Adeq Precision, at 10.29, surpasses the desirable threshold of 4, demonstrating the model's ability to provide reliable insights in navigating the design space.

The Model F-value of 19.51 underscores the significance of the model, with only a 0.04% probability of such a large F-value because of noise, confirming its validity. Significant model terms, including A, B, AB, AC, BC, A^2, B^2, and C^2, with *p-values* below 0.05, highlight their importance in the model. The Lack of Fit F-value of 0.82, along with its insignificance relative to pure error and a 54.6% chance due to noise,

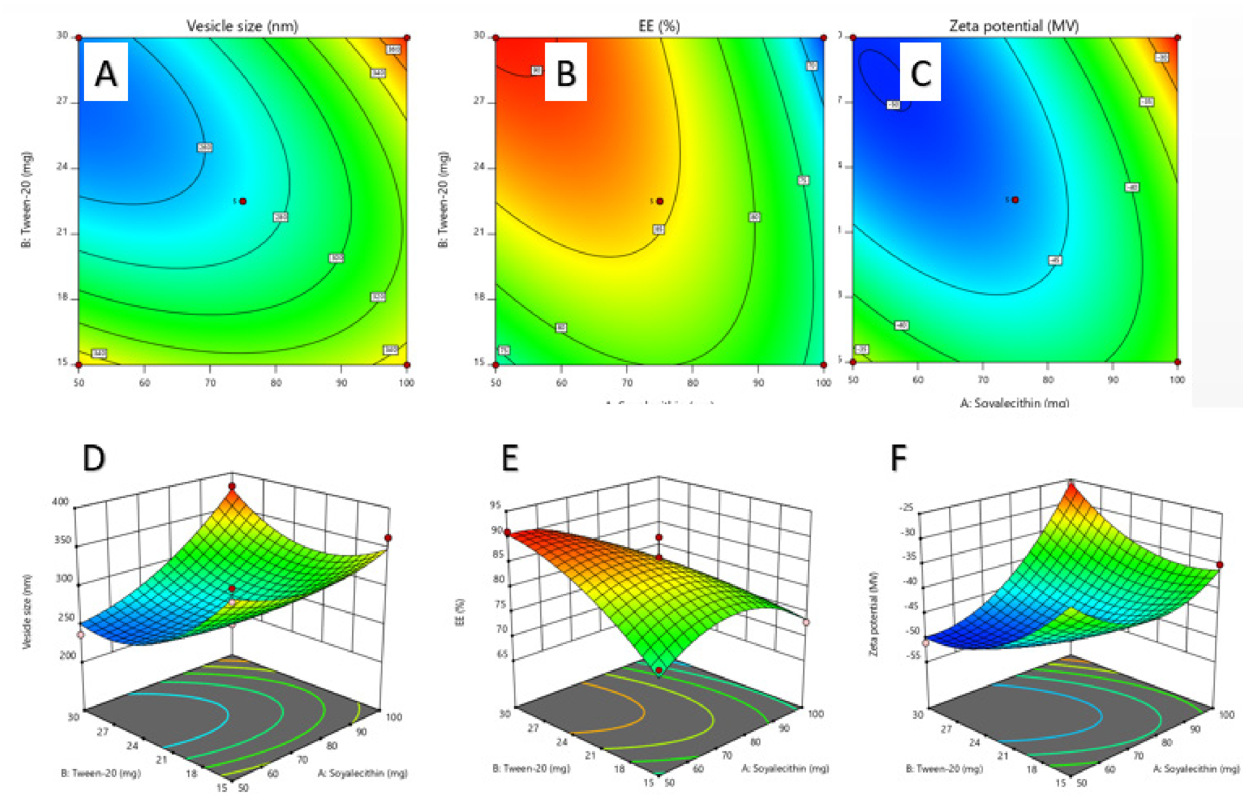

Figure 4: Contour plots illustrate the responses of A) vesicular size, B) entrapment efficiency, and C) zeta potential, while 3D plots depict the responses of D) vesicular size, E) entrapment efficiency, and F) zeta potential

Table 2: The equations for Y_1, Y_2, and Y_3 for the quadratic model

Equations of the responses
Y_1=+269.8+30.88A-17.37B-42.75C+32AB-27.75AC+18.75BC+22.6A²+39.6B²-10.15C²
Y_2=+85.60-6.00A+2.5B+0.00C-6.0AB+0.00AC-8.5BC-6.55A²-3.05B²-6.05C²
Y_3= -47.4+5.37A-1.5B+1.63C+6.75AB-0.50 AC+5.75BC+6.45A²+4.70B²+7.95C²

suggests a well-fitting model capable of capturing underlying relationships effectively. Both the Predicted R^2 (0.7290) and Adjusted R^2 (0.9124) exhibit reasonable agreement, indicating consistent predictive power across datasets. Adeq Precision, exceeding the desirable threshold at 12.55, illustrates the model's reliability in providing valuable insights for navigating the design space.

The Model F-value of 39.96 emphasizes the significance of the model, with only a 0.01% chance of such a large F-value occurring due to noise, confirming its validity. Significant model terms, including A, B, AB, AC, BC, A^2, B^2, and C^2, with p-values below 0.05, underscore their importance in the model. The Lack of Fit F-value of 0.45, along with its insignificance relative to pure error and a 73.36% chance due to noise, suggests a well-fitting model capable of effectively capturing underlying relationships. Both the predicted R^2 (0.9011) and adjusted R^2 (0.9564) exhibit reasonable agreement, indicating consistent predictive power across datasets. Adeq Precision, surpassing the desirable threshold at 17.462, illustrates the model's reliability in providing valuable insights for navigating the design space (Table 2).

The provided equations in Table 2, represent mathematical models describing the association between the IV (X_1, X_2, and X_3) and the DV (Y_1, Y_2, and Y_3) in the experimental design. These equations are derived from experimental data and are useful for predicting the DV based on specific combinations of the IV. Each equation consists of various coefficients representing the linear, interaction, and quadratic effects of the IV on the DV. By analyzing these equations, one can understand how changes in the IV affect the responses of interest, providing valuable insights for optimizing the experimental conditions to achieve desired outcomes.

The contour plots presented in Figures 4A, 4B, and 4C provide a graphical representation of the relationship between the IV and DV. These plots offer valuable insights into how changes in the levels of the IV influence the values of the DV. By analyzing the contour plots, one can identify regions of the parameter space where the DVs are optimized, facilitating the selection of optimal situations for achieving desired outcomes.

In addition, the 3D plots depicted in Figures 4D, E, and F offer a visual depiction of the interaction between multiple IV and their impact on the DV. These plots provide a full indulgent of the association between the variables by illustrating how changes in one or more IVs affect the behavior of the DV. By examining the 3D plots, researchers can identify complex patterns of interaction between the variables and pinpoint

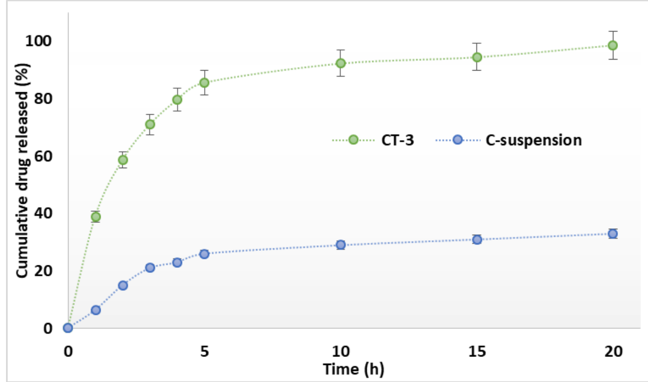

Figure 5: Comparing the performance of optimized transferosomes (CT-3) with Captopril suspension

optimal parameter settings for maximizing vesicular size, entrapment efficiency, and zeta potential. Overall, the contour and 3D plots serve as powerful tools for visualizing and interpreting the results of the experimental design, aiding in the optimization of formulation conditions for CPL transferosomes (Figure 5).

The comparison is depicted in Figure 5 between optimized CPL transferosomes (CT-3) and C-suspension highlights significant differences in drug discharge kinetics and plasma concentrations. Notably, CT-3 demonstrates extended drug discharge profiles, suggesting sustained and controlled drug discharge over time, contrasting with the rapid discharge observed with CPL suspension. This prolonged drug discharge pattern exhibited by CT-3 is indicative of its potential to maintain therapeutic drug levels in the bloodstream for an extended duration, offering aids in terms of effectiveness and patient acquiescence. The higher plasma concentrations achieved with CT-3 compared to CPL suspension underscore the improved bioavailability of the drug when delivered via transferosomes. The sustained drug discharge from transferosomes can be attributed to their unique structural properties, including the encapsulation of CPL within vesicles. This encapsulation enables a controlled discharge mechanism, where the drug is gradually discharged from the vesicles, leading to sustained drug levels in the systemic circulation. Overall, the findings suggest that CT-3, with its extended drug discharge profile and enhanced bioavailability, holds promise as a potential therapeutic delivery system for CPL, offering advantages in the management of heart problems.

CONCLUSION

In conclusion, the *in-vitro* and *ex-vivo* permeation studies have provided compelling evidence that transferosomal formulations markedly enhance drug permeation compared to plain CPL suspension. This enhanced permeation is indicative of the superior efficiency of transferosomes in enabling drug delivery through biological barriers. The findings suggest that CPL transferosomes are a highly promising delivery system capable of achieving prolonged and controlled drug discharge. This capability is particularly significant in the context of hypertension management, where consistent and controlled drug discharge can lead to better regulation of blood pressure and improved patient adherence to medication regimens. The potential improvements in therapeutic outcomes, owing to the advanced delivery characteristics of transferosomal formulations, underscore their importance in the development of more effective hypertension treatments. Overall, the success of CPL transferosomes in these studies points to their significant potential for clinical application, offering a pathway to enhance the efficacy and reliability of hypertension management strategies.

ACKNOWLEDGMENTS

None.

REFERENCES

1. Ahad HA, Haranath C, Anoohya A, Tejaswini J, Veeresh K. Drug Tragedies: The Dark Epoch of Clinical Prosecutions That Made Manhood Mysterious Fatalities. pharmaceuticals. 1982;500:2009.
2. Groenewegen A, Rutten FH, Mosterd A, Hoes AW. Epidemiology of heart failure. European journal of heart failure. 2020;22(8):1342-56.
3. Ahad HA, Haranath C, Pradeepkumar B, Vinay C, Reddy CYCS, Sajid MS, et al. Organ transplantation, pros, cons, and illustrations: a basic awareness to the public. Abasyn Journal of Life Sciences. 2021;4(1):168-74.
4. Devhare LD and Gokhale N. Antioxidant and Antiulcer Property of Different Solvent Extracts of Cassia Tora Linn. Research Journal of Pharmacy and Technology. 2022;15(3);1109-1113.
5. Tiwari R, Mishra J, Devhare LD and Tiwari G. An updated review on recent developments and applications of fish collagen. Pharma Times. 2023;55(6):28-36
6. Ahad HA, Kiranmaye N, Yasmeen R, Ruksana H, Muneer S. Designing and Evaluation of Glimepiride Ficus glomerata Fruit Mucilage Matrix Transdermal Patches. Asian Journal of Chemistry. 2010;22(4):2935.
7. Shravani Y, Ahad HA, Haranath C, gari Poojitha B, Rahamathulla S, Rupasree A. Past Decade Work Done On Cubosomes Using Factorial Design: A Fast Track Information for Researchers.. (2021). Int J Life Sci Pharma Res.11(1):P124-35.
8. Anil K. Adimulapu, Lalchand D. Devhare, Anasuya Patil, Nilesh O. Chachda, G. Dharmamoorthy(2023). Design and Development of Novel Mini Tablet Cap Technology for the Treatment of Cardiovascular Diseases. International Journal of Drug Delivery. Technology. 2023;13(3):801-806
9. Chawla A, Devhare LD, Dharmamoorthy G, Ritika, Tyagi S. Synthesis and In-vivo Anticancer Evaluation of N-(4-oxo-2-(4-((5-aryl-1,3,4 thiadiazole-2yl) amino) Phenyl thiazolidine-3-yl) Benzamide derivative. International Journal of Pharmaceutical Quality Assurance. 2023;14(3):470-474.
10. Jyothika LSK, Ahad HA, Haranath C, Kousar S, pal Gowd HD, Sadiya SH. Lakunde Sathish Kumar Jyothika*, Hindustan Abdul Ahad, Chinthaginjala Haranath, Shaik Kousar, Hothur Dharani pal Gowd, Sampathikota Halima Sadiya. Research Journal of Pharmaceutical Dosage Form and Technology. 2022:157-62.
11. Eltahir AKAE, Ahad HA, Haranath C, Meharajunnisa B, Dheeraj S, Sai BN. Novel Phytosomes as Drug Delivery Systems and its Past Decade Trials. 2023.
12. Gnana RPM, Devhare LD, Dharmamoorthy G, Khairnar MV, Prasidha R. Synthesis, Characterisation, Molecular Docking Studies and Biological Evaluation of Novel Benzothiazole Derivatives as EGFR Inhibitors for Anti-breast Cancer Agents. International Journal of Pharmaceutical Quality Assurance. 2023;14(3):475-480.
13. Sonule M, Devhare LD, Babu MN, Gunjal SD, Varalaxmi S. Microemulgel-based Hydrogel of Diclofenac Sodium using Lipidium sativum as a Gelling Agent. International Journal of Drug Delivery Technology. 2023;13(4):1235-1239.
14. Shriram BK, Devhare LD, Mehrotra A, Deokar SS, Singh SP. Formulation and Evaluation of Mosquito Repellent Stick. International Journal of Drug Delivery Technology. 2023;13(4):1283-1286.
15. Sailaja KE, Pradeepkuma B. Nanovesicular transdermal delivery patches have previously had success: A beginning step toward a giant leap in drug delivery. NeuroQuantology. 2022;20(22):809.
16. Dong X, Fan J, Lin D, Wang X, Kuang H, Gong L, et al. Captopril alleviates epilepsy and cognitive impairment by attenuation of C3-mediated inflammation and synaptic phagocytosis. Journal of Neuroinflammation. 2022;19(1):226.
17. Riddiough GE, Walsh KA, Fifis T, Kastrappis G, Tran BM, Vincan E, et al. Captopril, a Renin–Angiotensin System Inhibitor, Attenuates Tumour Progression in the Regenerating Liver Following Partial Hepatectomy. International Journal of Molecular Sciences. 2022;23(9):5281.
18. Choudhary RK, Beeraka S, Sarkar BK, Dharmamoorthy G, Devhare L. Optimizing Verapamil Hydrochloride In-situ Delivery: A Strategic Formulation Approach using Box-Behnken Design for Enhanced Performance and Comprehensive Evaluation of Formulation Parameters. International Journal of Drug Delivery Technology. 2024;14(1):61-70.
19. Fouziya B, Hindustan AA, Dontha SC, Jagarlamudi SV, Reddy UC, Reddy PN. Fabrication and evaluation of cefpodoxime proxetil niosomes. Asian Journal of Pharmacy and Technology. 2022;12(2):109-12.
20. Abdul AH, Bala AG, Chintaginjala H, Manchikanti SP, Kamsali AK, Dasari RRD. Equator assessment of nanoparticles using the design-expert software. International Journal of Pharmaceutical Sciences and Nanotechnology (IJPSN). 2020;13(1):4766-72.
21. Abd El-Alim SH, Kassem AA, Basha M, Salama A. Comparative study of liposomes, ethosomes and transfersomes as carriers for enhancing the transdermal delivery of diflunisal: in vitro and in vivo evaluation. International journal of pharmaceutics. 2019;563:293-303.
22. Kumar KK, Kiran V, Choudhary RK, Devhare LD, Gunjal SD. Design Development and Characterization of Nicardipine Solid Lipid Nano-Particulars. International Journal of Drug Delivery Technology. 2024;14(1):71-78.
23. Priya MGR, Prasanth LML, Devhare LD, Yazdan SK, Gunjal S. Synthesis, DNA Binding, Molecular Docking and Anticancer Studies of Copper (II), Nickel (II), and Zinc (II) Complexes of Primaquine-based Ligand. International Journal of Pharmaceutical Quality Assurance. 2024;15(1):69-75.
24. Mundarinti SHB, Ahad HA. Impact of Pistacia lentiscus plant gum on particle size and swelling index in central composite designed amoxycillin trihydrate mucoadhesive microspheres. Indian Journal of Pharmaceutical Education and Research. 2023;57:763-72.
25. Kaur N, Yadav K, Garg R, Saroha K, Yadav D. Formulation and in vitro characterization of ketoconazole span 80 based

transfersomes gel, its comparison with liposomal gel and evaluation of antimicrobial activity. Journal of Bionanoscience. 2016;10(3):191-204.

26. Uplanchiwar VP, Raut SY, Devhare LD, et al. Pharmacological Assessment of Antiulcer Activity of Gloriosa Superba Linn Tubers In Experimentally Induced Gastric Ulcers. Journal of Medical Pharmaceutical and Allied Science. 2021;10(3);2852-2856.
27. Harsha SS, Ahad HA, Haranath C, Dasari RR, Gowthami M, Varam NJ, et al. Exfoliation technique of composing and depictions of clopidogrel bisulphate afloat microspheres. Journal of Evolution of Medical and Dental Sciences. 2020;9(14):1156-61.
28. Sultana SS, Krishna Sailaja A. Formulation and evaluation of diclofenac sodium transferosomes using different surfactants by thin film hydration method. Der Pharmacia Lettre. 2015;7(11):43-53.